NIES-GOSAT2-ALG-20191008-008-01

GOSAT-2 TANSO-CAI-2 L2 Pre-processing Algorithm Theoretical Basis Document

November 2020

National Institute for Environmental Studies
GOSAT-2 Project

HASHIMOTO Makiko[1)]
SHI Chong[1)]

1) Earth Observation Research Center (EORC), Japan Aerospace Exploration Agency (JAXA)

Revision History

Version	Revised on	Page	Description
00	May 2020	-	-
01	Nov. 2020	p.5, p.15	Modified the formulas

Table of Contents

1 Introduction

This Algorithm Theoretical Basis Document (ATBD) explains an algorithm of "TANSO-CAI-2 Level 2 (L2) pre-processing" to derive the apparent reflectance and surface albedo required for deriving "TANSO-CAI-2 L2 Cloud Discrimination and Aerosol Property Products".

1.1 Scope of the algorithm

Figure 1.1–1 shows the whole processing flow of GOSAT-2 data analysis. The scope of application in this ATBD is the yellow-colored part in the figure.

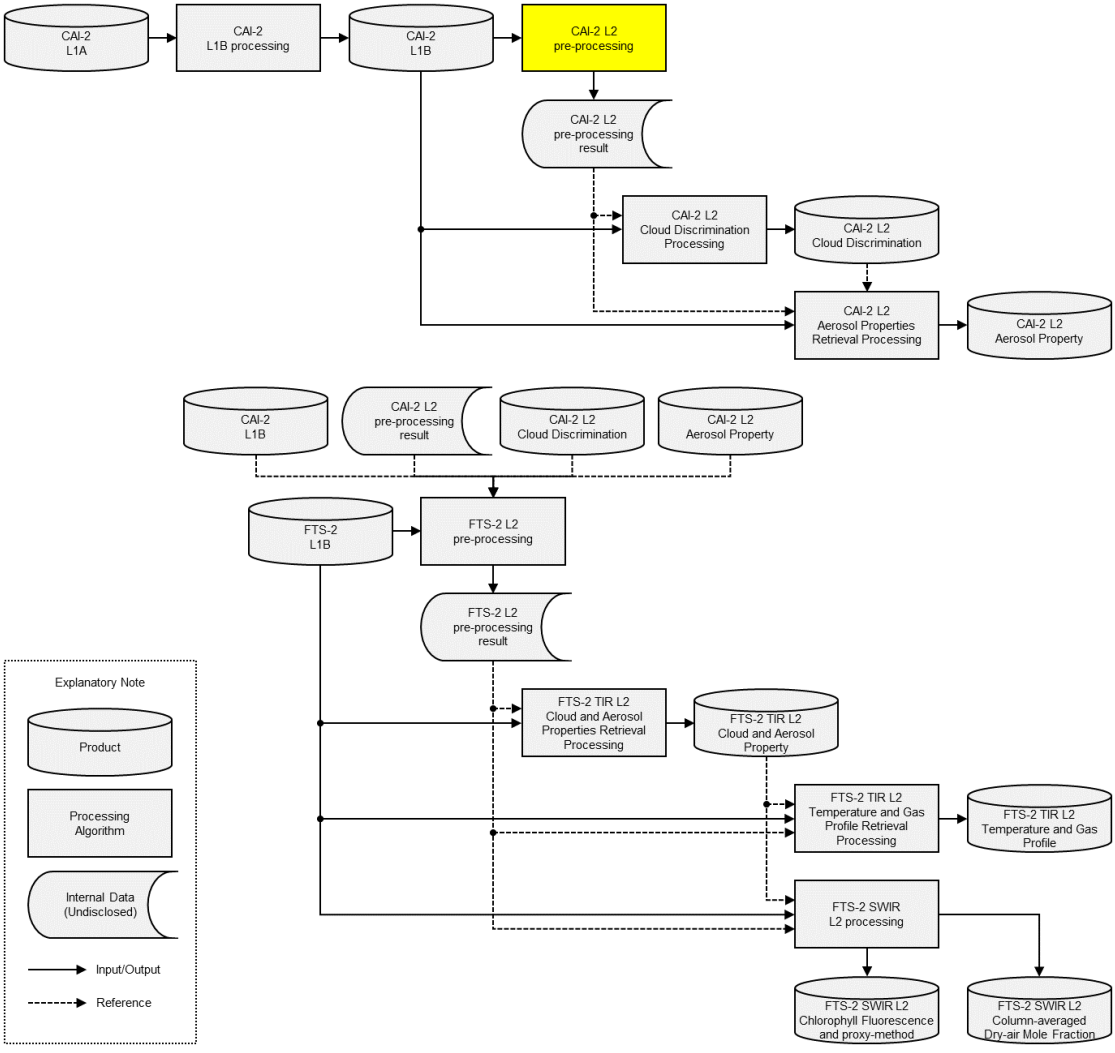

Figure 1.1–1. The scope of the algorithm described in this ATBD in the processing flow of GOSAT-2 data analysis.

1.2 Related documents

Related documents of the ATBD are as follows,

(1) GOSAT-2 TANSO-CAI-2 L1B Processing Algorithm Theoretical Basis Document
(2) GOSAT-2 TANSO-CAI-2 L2 Cloud Discrimination Processing Algorithm Theoretical Basis Document
(3) GOSAT-2 TANSO-CAI-2 L2 Aerosol Properties Retrieval Processing Algorithm Theoretical Basis Document

2 Background

This ATBD describes the conversion of CAI-2 Level 1B (L1B) radiance to apparent reflectance, minimum reflectance, and surface albedo as pre-process of CAI-2 L2 cloud discrimination and aerosol properties retrieval processings.

2.1 Overview of the GOSAT-2 sensors

Greenhouse gases Observing Satellite-2 (GOSAT-2) called "IBUKI-2", which is a subsequent satellite of GOSAT launched in 2009, was launched on October 29, 2018. The mission of GOSAT series is to measure the global concentration of greenhouse gases (GHG) in the atmosphere that is a cause of global warming. GOSAT-2 makes 89 laps a day, observing the whole globe in 6 days. GOSAT-2 has two sensors. One is Fourier Transform Spectrometer 2 (FTS-2) for GHG observation and the other is Cloud and Aerosol Imager 2 (CAI-2).
Table 2.1–1 shows the main specifications of CAI-2. The CAI-2 is a push-broom imaging sensor that has function of forward- and backward-viewings, consisting of seven wavelengths and ten bands from near ultraviolet (NUV), visible (VIS), near infrared (NIR), to short wavelength infrared (SWIR) as shown in Figure 2.1–1.

Table 2.1–1. Main specifications of CAI-2.

	Forward viewing					Backward viewing				
Band	1	2	3	4	5	6	7	8	9	10
Center of wavelength [μm]	0.339	0.441	0.672	0.865	1.630	0.377	0.546	0.672	0.865	1.630
Wavelength width [μm]	0.013	0.012	0.013	0.011	0.073	0.015	0.015	0.013	0.011	0.073
Resolution [m]	460				920	460				920
Effective pixels	Dummy pixels: 8 pixels Effective pixels: 2048 pixels				67–1024 pixels (256 pixels/ch)	Dummy pixels: 8 pixels Effective pixels: 2048 pixels				67–1024 pixels (256 pixels/ch)
Tilt angle [deg.]	+20					−20				
Swath [km]	920									

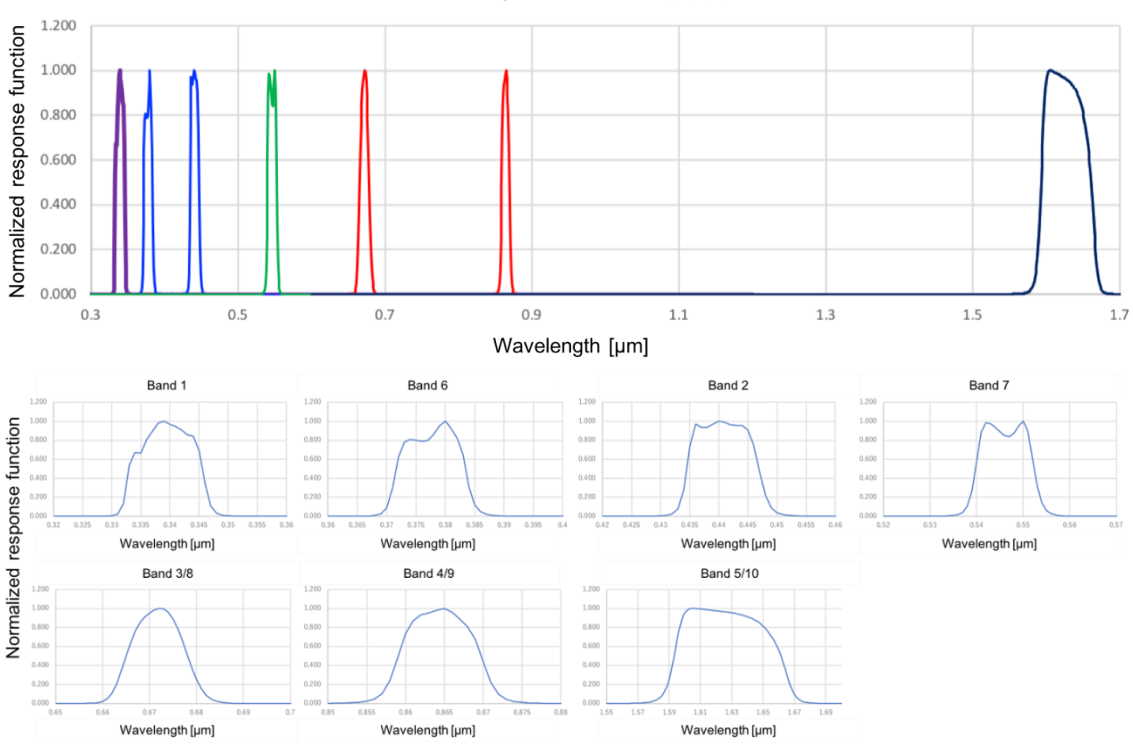

Figure 2.1–1. CAI-2 measurement wavelengths (top) and the normalized response function (bottom) of each band.

2.2 Overview of deriving surface albedo

This section describes how to derive the surface albedo, which is one of CAI-2 L2 pre-processing data. First, the satellite observation radiance data, L, is converted to apparent reflectance, R,

$$R = \frac{\pi L}{\mu_0 (F_0 / d^2)} \ , \tag{2.2-1}$$

where μ_0 is cosine of solar zenith angle, F_0 is the solar constant, and d is the distance between Earth and Sun in astronomical unit (AU). Next, the minimum reflectance data are selected from multiple day data before and after the analysis date. At this time, the second minimum reflectance and the first minimum reflectance are selected, and when the difference is larger than a threshold, the first minimum reflectance is judged to be affected by cloud shadows, and the second minimum reflectance is used as minimum reflectance. [Fukuda et al., 2013]. Assuming that there is no aerosol in the minimum reflectance data, the surface albedo is derived by performing a correction removing the influence of atmospheric molecular scattering (Rayleigh scattering).

The reflectance R_{sat} observed by the satellite can be expressed as follows using the reflection from the atmosphere (path radiance), R_{atmos}, the reflection due to the interaction between the ground and atmosphere, R_{ground}, and the transmission by the light absorbing gas.

$$R_{sat} = T_{gas}^2 \cdot (R_{atmos} + R_{ground}) \ , \tag{2.2-2}$$

$$R_{atmos} = R_{single} + R_{multiple} \ , \tag{2.2-3}$$

$$\begin{aligned} R_{ground} &= t(\tau;\mu_0) A_g t(\tau;\mu_1) + t(\tau;\mu_0) A_g r(\tau) A_g t(\tau;\mu_1) + \cdots \\ &= \frac{t(\tau;\mu_0) A_g t(\tau;\mu_1)}{1 - A_g r(\tau)} \end{aligned} \ , \tag{2.2-4}$$

$$t(\tau;\mu_0) = \frac{1}{\mu_0 F_0} \int_0^{2\pi} \int_0^1 L(\tau;\mu_0,\phi_0;\mu,\phi) \mu d\mu d\phi \ \ , \text{when } A_g = 0 \ , \tag{2.2-5}$$

$$r(\tau) = \frac{1}{\mu_0 F_0} \int_0^1 \int_0^{2\pi} \int_0^1 \int_0^{2\pi} L(\tau;\mu,\phi;\mu',\phi') \mu d\phi' d\mu' d\phi d\mu \ \ , \text{when } A_g = 0 \ , \tag{2.2-6}$$

where A_g is the surface albedo, τ is the optical thickness of the atmosphere. $t(\tau;\ \mu_0)$ is called unidirectional transmittance, and $r(\tau)$ is called spherical albedo. μ_0 and μ_1 are cosines of solar and satellite zenith angles, respectively. Using these equations, the surface albedo, A_g is given as follow,

$$A_g = \frac{1}{C + r(\tau)} \ , \tag{2.2-7}$$

$$C = \frac{t(\tau;\mu_0) t(\tau;\mu_1)}{R_{sat} / T_{gas}^2 - R_{atmos}} \ . \tag{2.2-8}$$

01

01

3 Input and output data

This chapter describes input and output data and reference data used for the analysis.

3.1 Input data

Table 3.1–1 lists the input data defined as "CAI-2 L1B product".
The surface albedo is derived from the CAI-2 L1B products, [$X_{day} - n_1$, $X_{day} + n_2$], one month before and after the analysis date X_{day}. The n_1 and n_2 are given as follows:

- n_1 = the number of required scenes 6 days before the analysis day
- n_2 = the number of required scenes 6 days after the analysis day

Pixels of different analysis dates are selected by nearest neighbor method using the latitude and longitude information based on the analysis date (X_{day}).

Table 3.1–1. Input data (from CAI-2 L1B product).

No.	Referrer	Data index	Unit
3.1–1	CAI-2 L1B (Forward viewing)	Calibrated radiance (Band 1–5)	[W/m^2/str/μm]
3.1–2	CAI-2 L1B (Forward viewing)	Solar zenith angle	[deg.]
3.1–3	CAI-2 L1B (Forward viewing)	Satellite zenith angle	[deg.]
3.1–4	CAI-2 L1B (Forward viewing)	Solar azimuth angle	[deg.]
3.1–5	CAI-2 L1B (Forward viewing)	Satellite azimuth angle	[deg.]
3.1–6	CAI-2 L1B (Forward viewing)	Geodetic latitude	[deg.]
3.1–7	CAI-2 L1B (Forward viewing)	Geodetic longitude	[deg.]
3.1–8	CAI-2 L1B (Forward viewing)	Solar distance	[AU]
3.1–9	CAI-2 L1B (Forward viewing)	Land/Water mask [0/1]*	—
3.1–10	CAI-2 L1B (Backward viewing)	Calibrated radiance (Band 6–10)	[W/m^2/str/μm]
3.1–11	CAI-2 L1B (Backward viewing)	Solar zenith angle	[deg.]
3.1–12	CAI-2 L1B (Backward viewing)	Satellite zenith angle	[deg.]
3.1–13	CAI-2 L1B (Backward viewing)	Solar azimuth angle	[deg.]
3.1–14	CAI-2 L1B (Backward viewing)	Satellite azimuth angle	[deg.]
3.1–15	CAI-2 L1B (Backward viewing)	Geodetic latitude	[deg.]
3.1–16	CAI-2 L1B (Backward viewing)	Geodetic longitude	[deg.]
3.1–17	CAI-2 L1B (Backward viewing)	Solar distance	[AU]
3.1–18	CAI-2 L1B (Backward viewing)	Land/Water mask [0/1]*	—
3.1–19	CAI-2 L1B (Backward viewing)	Forward pixel index	—

* Land/Water mask [0: Land, 1: Water surface]

3.1.1 Definition of input geometries

The geometry definition of the forward model (the radiative transfer calculation) is shown in Figure 3.1.1–1. In the forward model in the analysis, the solar zenith angle, θ_0, satellite zenith angle, θ, and relative azimuth angle, ϕ, are transformed from the observation angles using Eqs. (3.1.1–1) to (3.1.1–4).

$$\theta_0 = solar\_zenith\_angle_{L1B} \ , \tag{3.1.1-1}$$

$$\theta = satellite\_zenith\_angle_{L1B} \ , \tag{3.1.1-2}$$

$$d\phi = |satellite\_azimuth\_angle_{L1B} - solar\_azimuth\_angle_{L1B}| \ , \tag{3.1.1-3}$$

$$\phi = \begin{cases} 180 - d\phi, \text{when } d\phi \leq 180 \\ d\phi - 180, \text{when } d\phi > 180 \end{cases} \ , \tag{3.1.1-4}$$

where $0 \leq \phi \leq 180$.

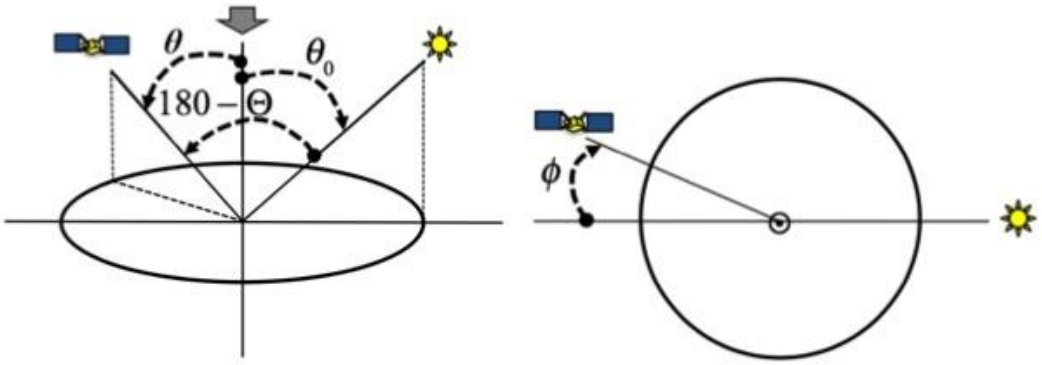

Figure 3.1.1–1. Geometries for the forward model (radiative transfer calculation) in the analysis. θ_0, solar zenith angle; θ, satellite nadir angle; and ϕ, relative azimuth angle.

3.2 Output data

Table 3.2–1 lists output data defined as “CAI-2 L2 pre-processing results”.

Table 3.2–1. Output data (CAI-2 L2 pre-processing results).

No.	Output destination	Data item	Unit
3.2–1	CAI-2 L2 pre-processing result (Forward viewing)	Apparent reflectance (Band 1–5)	—
3.2–2	CAI-2 L2 pre-processing result (Forward viewing)	Reflectance before atmospheric correction (Band 1–5)	—
3.2–3	CAI-2 L2 pre-processing result (Forward viewing)	Surface albedo (Band 1–5)	—
3.2–4	CAI-2 L2 pre-processing result (Backward viewing)	Apparent reflectance (Band 6–10)	—
3.2–5	CAI-2 L2 pre-processing result (Backward viewing)	Reflectance before atmospheric correction (Band 6–10)	—
3.2–6	CAI-2 L2 pre-processing result (Backward viewing)	Surface albedo (Band 6–10)	—

3.3 Reference data

Table 3.3–1 lists input data other than the input data in Section 3.1, which is called reference data here.

Table 3.3–1. Reference data used in the algorithm.

No.	Referrer	Data index	Data information	Unit
3.3–1	JRA-55	Total ozone	Model grid data/Total column forecast fields (1.25° × 1.25° grid)	[DU]
3.3–2	JRA-55	Pressure	Model grid data/surface analysis fields (1.25° × 1.25° grid)	[Pa]
3.3–3	JRA-55	Precipitable water	Model grid data/surface analysis fields (1.25° × 1.25° grid)	[kg m^{-2}]
3.3–4	JRA-55	Relative humidity (2m)	Model grid data/surface analysis fields (1.25° × 1.25° grid)	[%]
3.3–5	JRA-55	Specific humidity	Model grid data/surface analysis fields (1.25° × 1.25° grid)	[kg kg^{-1}]
3.3–6	CAI-2 instrument information	Radiance calibration factor	Slope and offset for each band (Update several month)	—
3.3–7	Thuillier (2003)	Solar constant	Fix (Calculated with response function)	[$W/m^2/\mu m$]

3.3.1 JRA-55 meteorological data

The Japanese 55-years reanalysis (JRA-55) is used for the analysis. In this analysis, surface analysis fields and total column forecast fields data are used as meteorological data (Table 3.3–1). The model grid size is 1.25 degrees and there are every three or six hours data. For the CAI-2 aerosol analysis, the closest grid to CAI-2 observed longitude and latitude and time is picked out by the nearest neighbor method. The unit and values of several variables are converted to be used in the aerosol retrieval analysis as shown in Table 3.3.1–1.

Table 3.3.1–1. Unit conversion of meteorological data (JRA-55) to use the aerosol retrieval.

Data index	Unit of JRA-55	Unit for the analysis	Equation
Total ozone	[DU]	[DU]	—
Pressure	[Pa]	[hPa]	3.3.1–1
Relative humidity (2m)	[%]	(0, 1)	3.3.1–2

JRA-55 pressure data, $press_{IN}$ at unit [Pa] is converted to $press_{OUT}$ at unit [hPa] for the aerosol retrieval.

$$press_{OUT} = press_{IN} \times 0.01 \ . \qquad (3.3.1-1)$$

JRA-55 relative humidity data, RH_{IN} at unit [%], is converted to RH_{OUT} at a range (0, 1) for the aerosol retrieval.

$$RH_{OUT} = RH_{IN} \times 0.01 \ . \qquad (3.3.1-2)$$

3.3.2 CAI-2 radiance calibration factor

The CAI-2 L1B radiance is calculated by the radiometric conversion coefficient based on the pre-flight test result. Radiance calibration factor is estimated by the vicarious calibration experiment for each band. The calibrated radiance is calculated by users using the radiance calibration factor as follows,

$$\begin{aligned} &\mathrm{Calibrated\_Radiance} \\ &= \mathrm{L1B\_Radiance} \times \mathrm{Calibration\_Factor\_slope} + \mathrm{Calibration\_Factor\_offset} \ . \end{aligned} \qquad (3.3.2-1)$$

3.3.3 Solar constant

Table 3.3.3–1 lists the values of the solar constant for the CAI-2 each band used in the algorithm. The solar constant calculated by using the solar constant in Thuillier (2003) and the CAI-2 response function (Figure 2.1–1).

Table 3.3.3–1. Solar constant for each band with CAI-2 response function.

Band	Wavelength [nm]	Solar constant [W/m^2/μm]
1	339	922.213
2	441	1837.52
3	672	1524.91
4	865	966.535
5	1630	237.898
6	377	1061.31
7	546	1862.60
8	672	1524.91
9	865	966.535
10	1630	237.898

4 CAI-2 L2 pre-processing algorithm

4.1 Overview of the algorithm

Figure 4.1–1 shows the flowchart of CAI-2 L2 pre-processing algorithm.

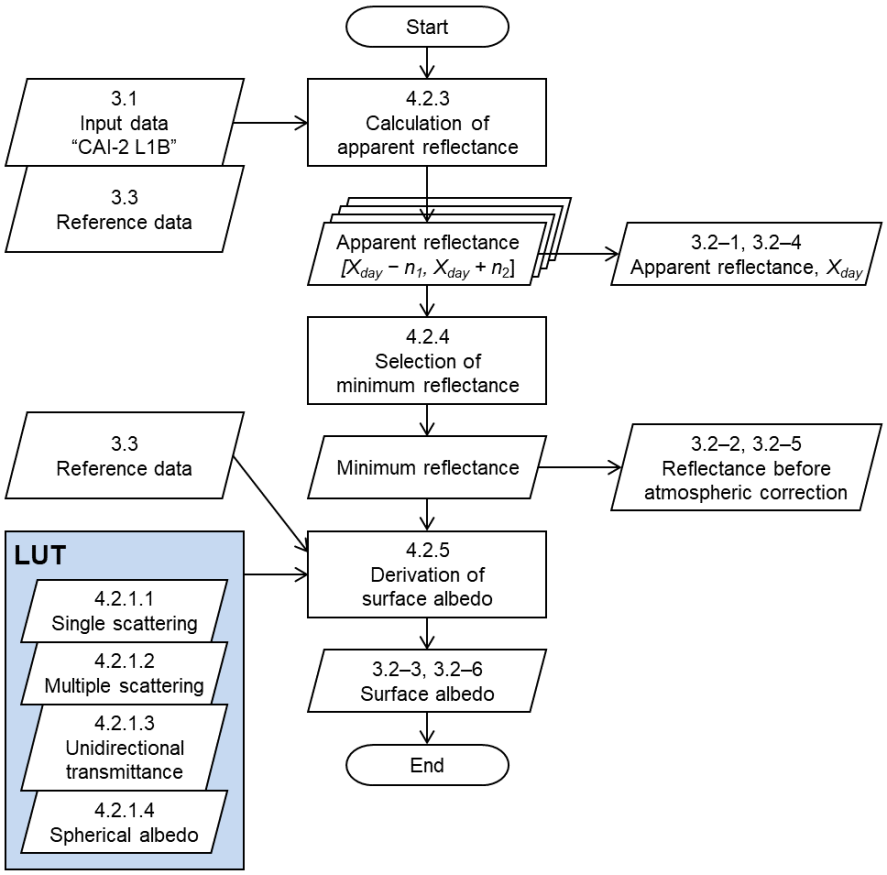

Figure 4.1–1. Algorithm flowchart of CAI-2 L2 pre-processing.

4.2 Data processing

4.2.1 Look-up table (LUT) in the algorithm

This section explains LUTs used in the algorithm. The LUTs refers to a table in which radiative transfer calculations are performed in advance to correct the influence of atmospheric molecular scattering required for deriving the surface albedo. There are four LUTs for atmospheric single scattering and multiple scattering components of reflectance, unidirectional transmittance, and spherical albedo. The LUTs have been created for all observation wavelengths. The LUTs are created in the condition in Table 4.2.1–1. Radiance, L, at each wavelength is calculated by Pstar that is a radiative transfer model with polarization [Ota et al., 2010], and LUTs are constructed by calculation described in SubSubsection 4.2.1.2 to 4.2.1.5. US standard atmospheric model are used.

Table 4.2.1–1. The condition to make LUTs.

		Num	Set values to make LUT
Wavelength [nm]	λ	7	339, 377, 441, 546, 672, 865, 1630
Solar zenith angle [deg.]	θ_0	29	0.0, 2.5, 5.0, 7.5, 10.0, 12.5, 15.0, 17.5, 20.0, 22.5, 25.0, 27.5, 30.0, 32.5, 35.0, 37.5, 40.0, 42.5, 45.0, 47.5, 50.0, 52.5, 55.0, 57.5, 60.0, 62.5, 65.0, 67.5, 70.0
Satellite zenith angle [deg.]	θ_1	25	0.0, 2.5, 5.0, 7.5, 10.0, 12.5, 15.0, 17.5, 20.0, 22.5, 25.0, 27.5, 30.0, 32.5, 35.0, 37.5, 40.0, 42.5, 45.0, 47.5, 50.0, 52.5, 55.0, 57.5, 60.0
Relative azimuth angle [deg.]	ϕ	46	0.0, 4.0, 8.0, 12.0, 16.0, 20.0, 24.0, 28.0, 32.0, 36.0, 40.0, 44.0, 48.0, 52.0, 56.0, 60.0, 64.0, 68.0, 72.0, 76.0, 80.0, 84.0, 88.0, 92.0, 96.0, 100.0, 104.0, 108.0, 112.0, 116.0, 120.0, 124.0, 128.0, 132.0, 136.0, 140.0, 144.0, 148.0, 152.0, 156.0, 160.0, 164.0, 168.0, 172.0, 176.0, 180.0
Pressure [hPa]	Prs	2	500, 1013.25

4.2.1.1 Single scattering component of reflectance for the atmosphere, R_{single}

The LUT of R_{single} is made in the condition of Table 4.2.1–1 when there is no aerosol in the atmosphere as follows,

$$R_{single} \approx \frac{\pi\omega\tau P(\Theta)}{\mu_0\mu_1} \ , \tag{4.2.1-1}$$

$$\omega = 1 \ , \tag{4.2.1-2}$$

$$\tau = \frac{Prs}{Prs_0} 0.008569\lambda^{-4\left(1+\frac{0.0113}{\lambda^2}+\frac{0.00013}{\lambda^4}\right)} \ , \tag{4.2.1-3}$$

$$Prs_0 = 1013.15 \text{ hPa} \ , \tag{4.2.1-4}$$

$$P(\Theta) = \frac{3}{16\pi}(1+\cos^2\Theta) \ , \tag{4.2.1-5}$$

$$\int_\Omega P(\Theta)d\Omega = 1 \ , \tag{4.2.1-6}$$

where ω, τ, and $P(\Theta)$ are the single scattering albedo, atmospheric optical depth, and phase function at a scattering angle, Θ, of the Rayleigh scattering, respectively. *Prs* and Prs_0 are the pressure at a certain height and surface, and Ω is the solid angle.

4.2.1.2 Multiple scattering element of reflectance in the atmosphere, $R_{multiple}$

The LUT of $R_{multiple}$ is made in the condition of Table 4.2.1–1 when there is no aerosol in the atmosphere, i.e., $\tau_{aero} = 0$, using the radiance calculated by Pstar code, L_{Pstar}, as follows,

$$\tau = \frac{Prs}{Prs_0} 0.008569 \lambda^{-4\left(1+\frac{0.0113}{\lambda^2}+\frac{0.00013}{\lambda^4}\right)} \ , \tag{4.2.1-7}$$

$$R_{Pstar}(\lambda, \theta_0, \theta_1, \phi) = \frac{\pi L_{Pstar}(\lambda, \theta_0, \theta_1, \phi)}{\mu_0 F_0} \ , \tag{4.2.1-8}$$

$$R_{multiple} = R_{Pstar}(\lambda, \theta_0, \theta_1, \phi, \tau_{aero} = 0) - R_{single} \ , \tag{4.2.1-9}$$

where λ, θ_0, θ_1, and ϕ are the wavelength, solar zenith angle, satellite zenith angle, and relative azimuth angle, respectively.

4.2.1.3 Unidirectional transmittance, $t(\tau; \mu_0)$

The LUT of $t(\tau; \mu_0)$ is made in the condition of Table 4.2.1–1 when there is no aerosol in the atmosphere, i.e., $\tau_{aero} = 0$, using apparent reflectance calculated by Pstar code, L_{Pstar}, as follows,

$$A_g = 0 \ , \tag{4.2.1-10}$$

$$\tau = \frac{Prs}{Prs_0} 0.008569 \lambda^{-4\left(1+\frac{0.0113}{\lambda^2}+\frac{0.00013}{\lambda^4}\right)} \ , \tag{4.2.1-11}$$

$$t(\tau; \mu_0) = \frac{1}{\mu_0 F_0} \int_0^{2\pi} \int_0^1 L_{Pstar}(\tau; \mu_0, \phi_0; \mu, \phi) \mu d\mu d\phi \ , \tag{4.2.1-12}$$

where A_g is the surface albedo.

4.2.1.4 Spherical albedo, $r(\tau)$

The LUT of $r(\tau)$ is made in the condition of Table 4.2.1–1 when there is no aerosol in the atmosphere, i.e., $\tau_{aero} = 0$, using apparent reflectance calculated by Pstar code, L_{Pstar} as follows,

$$A_g = 0 \ , \tag{4.2.1-13}$$

$$\tau = \frac{Prs}{Prs_0} 0.008569 \lambda^{-4\left(1+\frac{0.0113}{\lambda^2}+\frac{0.00013}{\lambda^4}\right)} \ , \tag{4.2.1-14}$$

$$r(\tau) = \frac{1}{\mu_0 F_0} \int_0^1 \int_0^{2\pi} \int_0^1 \int_0^{2\pi} L_{Pstar}(\tau; \mu, \phi; \mu', \phi') \mu d\phi' d\mu' d\phi d\mu \ . \tag{4.2.1-15}$$

4.2.2 Transmission of light absorbing gas

T_{gas} is calculated using Eq. (4.2.2–1) and the parameter in Table 4.2.2–1 for each wavelength.

$$T_{gas} = T_{O_3} = a \times O_3 \text{ [DU]} \ . \tag{4.2.2-1}$$

Table 4.2.2–1. The transformation factors from total ozone at unit DU to transmittance, T_{O_3}.

Wavelength [nm]	339	377	441	546	673	865	1630
a (P = 500 hPa)	1.437e−05	0.0	2.723e−06	7.884e−05	3.824e−05	1.584e−06	0.0
a (P = 1013.25 hPa)	1.523e−05	0.0	2.832e−06	8.167e−05	3.963e−05	1.640e−06	0.0

4.2.3 Apparent reflectance

The apparent reflectance, *R*, is calculated using the corrected CAI-2 L1B radiance, L'_{L1B}, by the calibration factors, *a* and *b* as follows,

$$R = \frac{\pi L'_{L1B}}{\mu (F_0/d^2)} \ , \tag{4.2.3-1}$$

$$L'_{L1B} = a \cdot L_{L1B} + b \ , \tag{4.2.3-2}$$

where μ_0 is the cosine of solar zenith angle, L_{L1B} is the original CAI-2 L1B radiance, F_0 and *d* are solar constant and the distance between Earth and Sun in AU.

4.2.4 Minimum reflectance and cloud shadow correction

The first or second minimum reflectance at Band 3 for forward viewing and Band 8 for backward viewing are selected as a minimum reflectance from about one-month data between $X_{day} - n_1$ and $X_{day} + n_2$ day, where X_{day} is an analysis day and n_1 and n_2 are the numbers of required scenes 6 days before and after the analysis day, respectively. When the difference between first and second minimum reflectances at Band 1 and Band 4 for forward viewing (Band 6 and Band 9 for backward viewing) is smaller and larger than the thresholds, $R_{Band1/6,t}$ and $R_{Band4/9,t}$ in Eqs. (4.2.4–4) and (4.2.4–5), respectively, the second minimum reflectance is selected as a minimum reflectance. The thresholds are given by an input file named “rmin.par”. Then, the second minimum reflectance is selected as the minimum reflectance, $R_{min,mod,Band3/8}$ and the first minimum reflectance is regarded as a cloud shadow [Fukuda et al., 2013]. For the other bands, the same day’s data with Band 3/8 are selected.

$$R_{min,mod,Band3/8} = \begin{cases} R_{2nd,min,Band3/8}, \text{if } (\Delta R_{Band1/6} < R_{Band1/6,t}) \text{ and } (\Delta R_{Band4/9} > R_{Band4/9,t}) \\ R_{1st,min,Band3/8}, \text{else} \end{cases} \ , \tag{4.2.4-1}$$

$$\Delta R_{Band1/6} = R_{2nd,min,Band1/6} - R_{1st,min,Band1/6} \ , \tag{4.2.4-2}$$

$$\Delta R_{Band4/9} = R_{2nd,min,Band4/9} - R_{1st,min,Band4/9} \ , \tag{4.2.4-3}$$

$$R_{Band1/6,t} = 0.10 \ , \tag{4.2.4-4}$$

$$R_{Band4/9,t} = 0.06 \ . \tag{4.2.4-5}$$

4.2.5 Derivation of surface albedo

The surface albedo at each wavelength is derived by removing the effect of atmospheric molecular scattering from the minimum reflectance as shown in Eqs. (4.2.5–1) and (4.2.5–2). Note that no aerosol is assumed in the atmosphere at minimum reflectance.

$$A_g = \frac{1}{C + r_{Band(i)}(\tau)} \ , \qquad (4.2.5-1)$$

$$C = \frac{t_{Band(i)}(\tau;\mu_0)t_{Band(i)}(\tau;\mu_1)}{R_{Band(i)}(\mu_1,\mu_0,\phi)/T^2_{gas,Band(i)} - R_{atmos,Band(i)}(\mu_1,\mu_0,\phi)} \ , \qquad (4.2.5-2)$$

01

where μ_0, μ_1, and ϕ are solar zenith angle, satellite zenith angle, and relative azimuth angle, respectively. The subscript "*i*" denotes observation band number from 1 to 10. R_{atmos} (= R_{single} + $R_{multiple}$), t, r, and T_{gas} are obtained by LUTs.

5 Prerequisites and constraints

5.1 Definition of geometries used in the algorithm

Figure 5.1–1 shows the definition of observation geometry used in the algorithm.

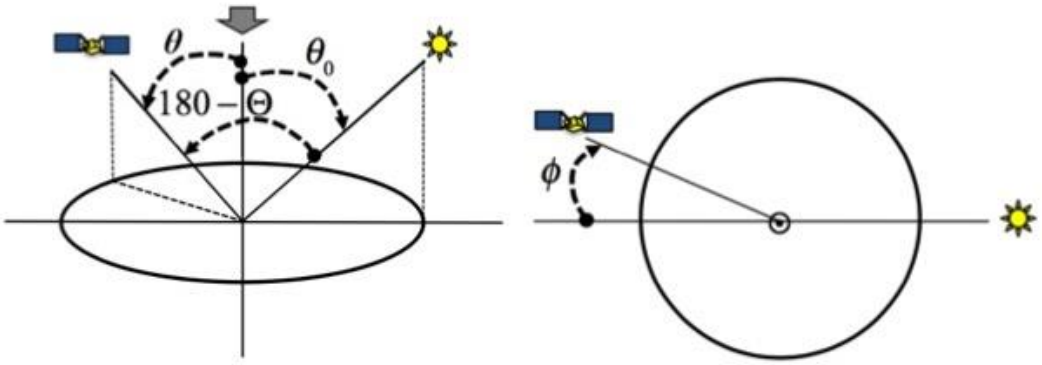

Figure 5.1–1. Definition of geometries used in the analysis. θ_0 solar zenith angle; θ, satellite zenith angle; and ϕ, relative azimuth angle. Note that $0 \leq \phi \leq 180$.

5.2 Processing range of deriving surface albedo

Surface albedo processing is applied to all scenes regardless of land or water.

5.3 Processing range of observation geometry

Processing is performed when the solar zenith angle is less than 85 degrees. Pixel data that does not satisfy the conditions is invalid.

5.4 Condition of selecting minimum reflectance

The first and second minimum reflectances are processed for the analysis when the number of valid data is N_{day} or more. Pixel data that does not satisfy the conditions is added a flag as invalid. The value of N_{day} is given by an input file named “rmin.par”, and basically $N_{day} = 5$.

References

Fukuda, S., T. Nakajima, H. Takenaka, A. Higurashi, N. Kikuchi, T. Y. Nakajima, and H. Ishida (2013), New approaches to removing cloud shadows and evaluating the 380 nm surface reflectance for improved aerosol optical thickness retrievals from the GOSAT/TANSO‐Cloud and Aerosol Imager, *J. Geophys. Res.*, **118**, 13520–13531, https://doi.org/10.1002/2013JD020090.

Ota,Y., A. Higurashi, T. Nakajima, and T. Yokota (2010), Matrix formulations of radiative transfer including the polarization effect in a coupled atmosphere–ocean system, *J. Quant. Spectrosc. Radiat. Transfer*, **111**, 878–894, https://doi.org/10.1016/j.jqsrt.2009.11.021.

Thuillier, G., M. Hersé, D. Labs, T. Foujols, W. Peetermans, D. Gillotay, P. C. Simon, and H. Mandel (2003), The Solar Spectral Irradiance from 200 to 2400 nm as Measured by the SOLSPEC Spectrometer from the ATLAS and EURECA Missions, *Sol. Phys.*, **214**, 1–22, https://doi.org/10.1023/A:1024048429145.